Heavy ion formation in Titan's ionosphere: Magnetospheric introduction of free oxygen and a source of Titan's aerosols?

E.C. Sittler Jr.[a,*], A. Ali[a,b], J.F. Cooper[a], R.E. Hartle[a], R.E. Johnson[c], A.J. Coates[d], D.T. Young[e]

[a] NASA Goddard Space Flight Center, MD, USA
[b] University of Maryland, College Park, MD, USA
[c] University of Virginia, Charlottesville, VA, USA
[d] Mullard Space Science Laboratory, UK
[e] Southwest Research Institute, San Antonio, TX, USA

ARTICLE INFO

ABSTRACT

Discovery by Cassini's plasma instrument of heavy positive and negative ions within Titan's upper atmosphere and ionosphere has advanced our understanding of ion neutral chemistry within Titan's upper atmosphere, primarily composed of molecular nitrogen, with $\sim$2.5% methane. The external energy flux transforms Titan's upper atmosphere and ionosphere into a medium rich in complex hydrocarbons, nitriles and haze particles extending from the surface to 1200 km altitudes. The energy sources are solar UV, solar X-rays, Saturn's magnetospheric ions and electrons, solar wind and shocked magnetosheath ions and electrons, galactic cosmic rays (GCR) and the ablation of incident meteoritic dust from Enceladus' E-ring and interplanetary medium. Here it is proposed that the heavy atmospheric ions detected in situ by Cassini for heights $>$950 km, are the likely seed particles for aerosols detected by the Huygens probe for altitudes $<$100 km. These seed particles may be in the form of polycyclic aromatic hydrocarbons (PAH) containing both carbon and hydrogen atoms C_nH_x. There could also be hollow shells of carbon atoms, such as C_{60}, called fullerenes which contain no hydrogen. The fullerenes may compose a significant fraction of the seed particles with PAHs contributing the rest. As shown by Cassini, the upper atmosphere is bombarded by magnetospheric plasma composed of protons, H_2^+ and water group ions. The latter provide keV oxygen, hydroxyl and water ions to Titan's upper atmosphere and can become trapped within the fullerene molecules and ions. Pickup keV N_2^+, N^+ and CH_4^+ can also be implanted inside of fullerenes. Attachment of oxygen ions to PAH molecules is uncertain, but following thermalization O+ can interact with abundant CH_4 contributing to the CO and CO_2 observed in Titan's atmosphere. If an exogenic keV O+ ion is implanted into the haze particles, it could become free oxygen within those aerosols that eventually fall onto Titan's surface. The process of freeing oxygen within aerosols could be driven by cosmic ray interactions with aerosols at all heights. This process could drive pre-biotic chemistry within the descending aerosols. Cosmic ray interactions with grains at the surface, including water frost depositing on grains from cryovolcanism, would further add to abundance of trapped free oxygen. Pre-biotic chemistry could arise within surface microcosms of the composite organic-ice grains, in part driven by free oxygen in the presence of organics and any heat sources, thereby raising the astrobiological potential for microscopic equivalents of Darwin's "warm ponds" on Titan.

1. Introduction

The Voyager 1 Titan flyby on November 12, 1980 showed a very complex encounter with Saturn's magnetosphere with an induced magnetotail (Ness et al., 1981) and a bite-out in the magnetospheric electron population for $E > 500$ eV (Bridge et al., 1981; Hartle et al., 1982). It was also shown that the upstream plasma was composed of light and heavy ions (Hartle et al., 1982; Sittler et al., 2004, 2005) and that the heavy ions (N^+ or O^+) had keV energies. The upstream magnetic field of $\sim$5 nT resulted in a heavy ion gyro-radii of $\sim$5000 km, which is larger than the size of Titan. A review of Cassini plasma and field observations of Titan's interaction is given by Coates (2009a). The atmosphere detected by Voyager was primarily composed of N_2, (Broadfoot et al., 1981) as predicted by Hunten (1977) and the small methane component was detected earlier by Kuiper (1944). Voyager also detected a complex suite of hydrocarbons and nitriles using the infrared spectrometer IRIS (Hanel et al., 1981, 1982). From these measurements exospheric models with H, H_2, N, CH_4 and N_2 were constructed (Hartle et al., 1982; Sittler et al., 2004, 2005) and

* Corresponding author. Tel.: +1 301 286 9215; fax: +1 301 286 1433.
E-mail address: Edward.C.Sittler@nasa.gov (E.C. Sittler Jr.).

complex neutral and ion chemistry was predicted to occur in its upper atmosphere and ionosphere (Yung et al., 1984; Yung, 1987; Toublanc et al., 1995; Cravens et al., 1997). Sittler et al. (2004, 2005) also predicted that the dominant pickup ion slowing the magnetospheric plasma flow is CH_4^+. The initial Cassini T_A flyby revealed a similar interaction to that of V1 but with the upstream heavy ion component uniquely identified as water group ions all of which contain oxygen. They also confirmed that the dominant pickup ion was CH_4^+ with some N_2^+ (Hartle et al., 2006a,b) as predicted (Sittler et al., 2004, 2005). The ion neutral mass spectrometer (INMS) instrument on Cassini during T_A encounter also detected a very complex neutral composition in Titan's upper atmosphere (Waite et al., 2005). During the T5 flyby INMS also detected a complex set of hydrocarbons which implied there was considerable ion chemistry occurring in this region (Cravens et al., 2006). The rich ion hydrocarbon chemistry extended up to ion mass ~100 amu. For later flybys when the spacecraft altitude dropped to 950 km Waite et al. (2007) reported the presence of benzene molecules plus heavy positive and negative ions with even higher masses. Coates et al. (2007) discovered heavy negative ions with mass ~4000 amu and higher. The number of heavy negative ions increased with decreasing altitude down to 950 km, the minimum altitude sampled by the Cassini spacecraft. Waite et al. (2007) and Coates et al. (2007) raised the possibility that the heavy ions were polycyclic aromatic hydrocarbons or PAHs.

The above discoveries pose the question why are we seeing heavy negative ions or PAHs at all. In the studies of interstellar clouds the presence of such molecules has a long history. Herbst (1981) first posed the question that negative molecular ions could exist in molecular clouds. In that paper the high electron affinities (>2 eV) for neutral free radicals and the large molecular size led to negative ion formation. Radiative attachment rate coefficients at cloud temperatures ~10–50 K can be as high as the collision rate $k \sim 10^{-7}$ cm^3/s. Later, Petrie and Bohme (2007) pointed out that there was no observational evidence for negative ions within molecular clouds, though their presence would be expected at low abundances. Subsequently McCarthy et al. (2006) combined radio observations of the star IRC+10 and molecular cloud TMC-1 and their recent laboratory measurements to detect the negative ion C_6H^-. This was later confirmed based on chemical models (Miller et al., 2007), which was then followed by detection of C_8H^- and C_4H^- in the molecular cloud TMC-1 (Brünken et al., 2007). C_8H^- was detected within the circumstellar envelope IRC+10 216 by Remijan et al. (2007). Sakai et al. (2007) detected C_6H^- within a low-mass star-forming region of L1527 and then later Sakai et al. (2008) reported the detection of C_4H^- near the low-mass Class 0 protostar IRAS 04368+2557. The anion C_3N^- was discovered within the interstellar medium (ISM) by Thaddeus et al. (2008). Then Herbst and Osamura (2008) performed quantum mechanical model calculations confirming on theoretical grounds the likely presence of the detected ion C_nH^-. They calculated high radiative attachment coefficients $>5 \times 10^{-8}$ cm^3/s that were similar to those measured by Miller et al. (2007). Relevant to the observations reported here, the observed negative ions C_nH^- have high carbon to hydrogen ratios ($n \geq 3$ with $n = 3$ having the lowest rate coefficient and $n = 8$ the highest rate coefficient (Herbst and Osamura, 2008).

In the case of Titan the ethynyl radical (C_2H) and benzene radical C_6H_5 (phenyl) can be important for the polymerization of PAHs (Goulay and Leone, 2006). At Titan the Cassini INMS instrument detected both acetylene (Waite et al., 2005) and benzene (Waite et al., 2007; Vuitton et al., 2009a) and their radicals C_2H (i.e., indirectly detected by Vuitton et al., 2009b) and C_6H_5 or phenyl by Vuitton et al. (2009a). Vuitton et al. (2007) also reported the detection of numerous hydrocarbons such as

polyynes (C_4H_2, C_6H_2, C_8H_2), possible detection of methylpolyynes (CH_3C_4H, CH_3C_6H) and benzene (C_6H_6). They also detected nitrogen bearing molecules cyanopolyynes (HC_3N, HC_5N), NH_3, methanimine (CH_2NH), nitriles (C_2H_3CN, C_2H_5CN) and possibly methylcyanopolyynes (CH_3C_3N, CH_3C_5N). Nitrogen bearing molecules can contribute to PAH formation and could thus be an important constituent of aerosols. The reader is referred to a comprehensive review article on PAH polymerization by Allamandola et al. (1989) the details of which are beyond the scope of this paper. The combination of recent detections of negative ions within molecular clouds and recent detections by Cassini of heavy negative ions at Titan suggests that there might be a connection between heavy negative ions and PAHs and/or fullerene formations. This does not mean that neutrals and positive ions do not also play an important role in the growth of heavier molecules since reaction rates for ion–neutral collision, involving either positive or negative ions, tend to be much faster than those for neutral–neutral collisions (e.g., Waite et al., 2007). However, as noted above, the radicals C_2H and C_6H_5 are probably also present at Titan, in which case growth of fullerenes and PAHs can also occur via neutral–neutral collisions (Goulay and Leone, 2006; Mebel et al., 2008; Bettens and Herbst, 1995). It is also true that acetylene and benzene can both lead to the growth of fullerenes and PAHs depending upon the chemical pathway taken (see Bettens and Herbst, 1995). The introduction of keV oxygen ions from Saturn's magnetosphere and their possible incorporation into fullerenes and possibly PAHs as discussed here, adds another dimension with strong exobiological implications. The present paper explores the implications of these two potentially related discoveries, upper atmospheric formation of the heavy negative ions and bombardment by keV oxygen ions for chemistry of Titan's atmosphere and surface.

2. Observations

2.1. Observations of heavy ions by Cassini

We begin this section by reviewing the relevant plasma observations of Titan's upper atmosphere and ionosphere made by the Cassini plasma spectrometer (CAPS) and ion neutral mass spectrometer (INMS) instruments. The first discovery of extremely heavy negative ions within Titan's ionosphere was made by the high time resolution observations of the CAPS electron spectrometer (ELS) during the T_A encounter and revealed a surprising population of heavy negative ions. These ions were subsequently observed on 15 other Titan encounters, and were analyzed by Coates et al. (2007) and initially reported by Waite et al. (2007). In all cases the negative ions observed near closest approach, were narrowly confined to the spacecraft ram direction, and contained distinct energy peaks (see Figs. 1 and 2 from Coates et al., 2007). During the spacecraft's flight through Titan's relatively cold ionosphere the spacecraft motion, ~6 km/s, provides an effective mass spectrometer feature for cold ionospheric ions. The conversion factor from ram energy to mass for singly charged ions at 6.0 km/s is $m_{amu} = 5.32 E_{ev}$ (Coates et al., 2007).

The CAPS instrument also has an ion beam spectrometer (IBS) primarily designed to measure high Mach plasma flows in the solar wind. But this instrument also provides good measurements of the positive ion component of Titan's ionosphere which, during these encounters, also appear as a high Mach flow in the spacecraft reference frame. This instrument has detected heavy positive ions (Waite et al., 2007). The mass of the positive ions extends up to several hundred amu but the detected ions are significantly less massive than the detected negative ions. Abundances of both the positive and negative ions peak at the lowest altitudes encountered (~950 km).

For T_A the observed maximum energy of the negative ions was ~60 eV, corresponding to an ion mass/charge m/q~320 amu/q. During other encounters, such as T16, the ion masses were as high as 10,000 amu/q as seen in Fig. 1 adpated from Coates et al. (2007). On various other encounters the ions were observed in rough mass groups at 10–30, 30–50, 50–80, 80–110, 110–200, (200–500, 500+) amu/q (Coates et al., 2007) because neither the ELS or IBS measure mass, but rather mass/charge. It was argued that these ions may in fact be multiply charged in this region of high electron density; therefore the actual mass could be up to five times higher. Such large highly charged ions provide seeds for forming aerosols (Coates et al., 2007, Waite et al, 2007). This relationship between mass and charge state is strongly tied to the assumed size of the ions with the following relationships. Waite et al. (2007) used φ~−2.5 kT/e ~0.027 V (T~125 K) based on the surface potential for a small dust grain with its corresponding charge $Q = 4\pi\varepsilon_0 a\varphi\exp(-a/\lambda_D)$ (ε_0 is permittivity of free space, a is grain's radius and λ_D is the Debye length). As discussed below, if the heavy ions are fullerenes, then the mean ion radius is estimated to be r_A~12 Å giving Q~1 and a maximum mass < 10,000 amu. If one uses for the heavy ions PAHs, then r_A~60 Å is possible so that Q~5 is estimated and very large ion masses become possible. Therefore, whether the heavy negative ions are fullerenes or PAHs becomes an important discriminator with regard to their true size.

As discussed in Coates et al. (2009b), negative ions were not anticipated this high in Titan's atmosphere and were not included in pre-Cassini chemical schemes (e.g., Wilson and Atreya, 2004) so that new chemical models are required. As noted earlier, ion–neutral collisions have high collision cross-sections, which in the case of the heavy ions approach the geometric cross-section (Waite et al., 2007). This allows such ions to grow rapidly in mass and size resulting in heavy ion formation. An important parameter in this growth process is the charge state. In case of negative ions this depends on the electron affinity of the molecule which as discussed below favors fullerenes.

The relationship between these ions and the heavy positive ion population was discussed by Waite et al. (2007, 2008). They suggested that nitrogen and methane in Titan's high atmosphere would be acted on by sunlight and magnetospheric particles forming heavier but relatively simple species by dissociation and ionization processes. Eventually this could lead to the growth of benzene and the other heavier ions detected by IBS up to ~350 amu/q (note that the upper limit could be set by the IBS detection threshold and even heavier positive ions could exist in substantial amounts). The growth process would continue to form heavier positive and negative ions. They suggested that these may be the tholins originally postulated by Sagan and Khare (1979). With continued growth these molecules could become large enough to be called aerosols and drift down towards Titan's surface. This chain of processes, initiated by magnetospheric interactions at the top of the atmosphere eventually affects the surface composition of Titan. This idea was supported by the extensive observations of negative ions by Coates et al. (2007).

Recently, further analysis of negative ion signatures has extended the number of encounters where negative ions were observed to 22 during Cassini's prime mission (Coates et al., 2009b). This allows a systematic study showing that the higher mass negative ions are observed preferentially as follows: (1) at low altitudes, with the highest mass (~10,000 amu/q) at Cassini's lowest altitude of 950 km, (2) at high Titan latitudes and (3) in the region of the terminator. On the basis of these results, Coates et al. (2009b) suggested that the formation of high mass negative ions is more efficient, or that destruction is less efficient when solar flux is highly attenuated. Coates et al. (2007) also suggested the possible ion identifications: (1) 10–20 amu/q CN^-, NH_2^- and O^-; (2) 30–50 amu/q NCN^-, $HNCN^-$ and C_3H^-; (3) 50–80 amu/q $C_5H_5^-$, C_6H^-, $C_6H_5^-$; and (4) mass groups 80–110, 110–200, 200–500 and
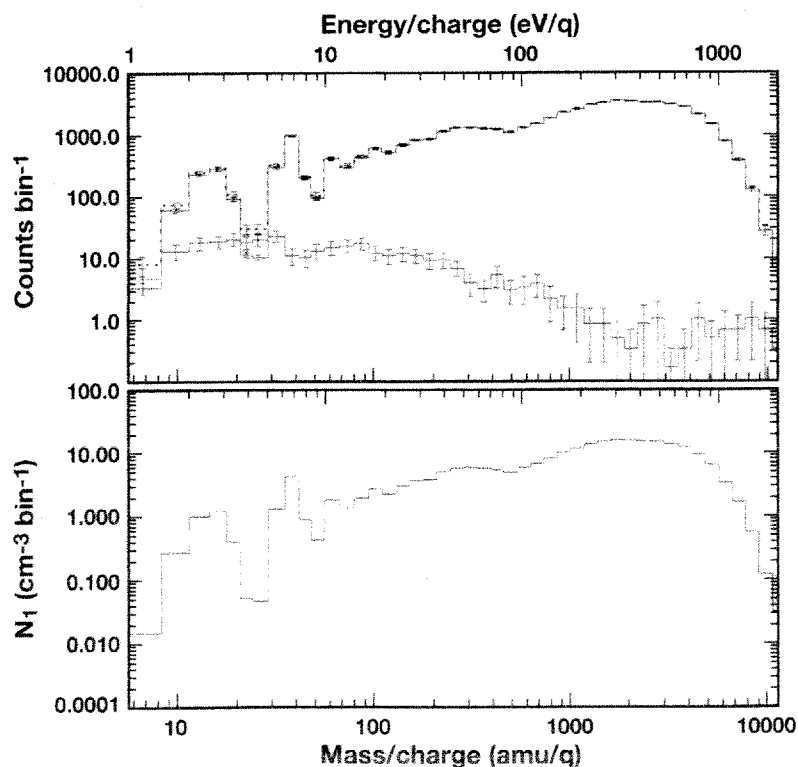

Fig. 1. Plot of CAPS-ELS ion counts versus ion energy (keV) or ion mass-per-charge (M/Q) from Coates et al. (2007) top panel and same for bottom panel except here we have ion density.

500–10,000 as polyynes, high order nitriles, PAHs and cyan aromatics. Nitrogen substitution PAHs are another possibility, but may not be stable in the UV environment of Titan's upper atmosphere. They may, however be stable in the haze layer of Titan's stratosphere at altitudes below 400 km (e.g., Ricca et al., 2001). More recently, Vuitton et al. (2009b) using a photochemical model have identified peaks in the CAPS-ELS mass spectrum at 22 ± 4 amu/q as CN^-/C_2H^-, 44 ± 8 amu/q as C_3N^-/C_4H^- and 82 ± 14 amu/q as C_5N^-. Most noteworthy is C_2H^- which is more abundant than CN^- below 850 km altitude in their model calculations. The fact that the ionization ratio for C_2H^-/C_2H is $\sim 2.4 \times 10^{-5}$ in their model shows that the free radical C_2H is likely present in Titan's upper atmosphere.

2.2. The formation of fullerenes and PAHs in Titan's upper atmosphere

As discussed in the papers by Coates et al. (2007, 2009b), and Waite et al. (2007, 2008) the heavy positive and negative ions could be evidence for the formation of PAHs ($C_{2n}H_x$) in Titan's ionosphere. The heavier ions are observed at lower altitudes with 950 km being the lowest altitude sampled by the Cassini space-craft. Vuitton et al. (2009a) have presented evidence of benzene in Titan's upper atmosphere with molar fractions $\sim 10^{-6}$ at 950 km altitude and levels higher than expected (see Lavvas et al., 2008a,b). Acetylene C_2H_2 has a molar abundance $\sim 10^{-3}$ at 1100 km (Vuitton et al., 2009b) and is more abundant than benzene (also see Shemansky et al., 2005; Waite et al., 2007). For atmospheric temperature like that at Titan, $T \sim 150$ K, one expects acetylene and benzene to lead to the formation of fullerenes and PAHs, respectively.

Laboratory measurements at much higher temperatures can produce fullerenes using low pressure benzene-oxygen flames (Gerhardt et al., 1987; Richter and Howard, 2000). PAHs can be formed in the laboratory using low pressure acetylene-oxygen flames (see Gerhardt et al., 1987). As discussed below at lower temperatures $T < 300$ K the reverse is true. There is a lot of free energy within Titan's upper atmosphere from bombarding high-energy photons (UV/EUV and X-rays) and magnetospheric charged particles. This high-energy input results in high thermal electron temperatures $T_{ec} \sim 1000$ K (Wahlund et al., 2005) and hot suprathermal photoelectrons $T_{eh} \sim 20,000$ K (Hartle et al., 2006a,b; Coates, 2009a). But, the ion–neutral and neutral–neutral collisions that lead to the growth of the heavy ions occur for $T \sim 150$ K. The high electron temperatures may affect ion charge state and formation of radicals. The above measurements were also made in oxygen flames, but Titan is essentially devoid of oxygen except for low abundances of CO, CO_2 and H_2O within Titan's atmosphere. Therefore, we feel these earlier laboratory measurements are not applicable to Titan.

More relevant to the observations at Titan fullerene and PAH formation occur under space environmental conditions within interstellar and circumstellar environments that more closely resemble Titan's upper atmosphere (e.g., Bohme, 1992). X-ray crystallography measurements have shown fullerenes to be hollow carbon cages (see Fig. 2) made of 60 carbon atoms C_{60} (720 amu) which have spherical shape or 70 carbon atoms C_{70} (840 amu) with ellipsoidal shape (Krätschmer, et al., 1990). The measured inner diameters are ~ 7 Å with effective mass density $\rho_F \sim 1.8$ gm/cm³ (i.e., mean radius $r \sim 5.4$ Å for $\rho \sim 2.25$ gm/cm³ for outer shell made of carbon with thickness ~ 3.4 Å). This should be compared to aerosol radii $r_A \sim 12.5$ nm estimated by Liang et al. (2007). Note, the $r_A \sim 260$ nm estimated by Waite et al. (2007) was an over estimate (Waite, 2008, private communication). Both C_{60} and C_{70} are known to be very stable (Kroto et al., 1985; Kroto et al.,
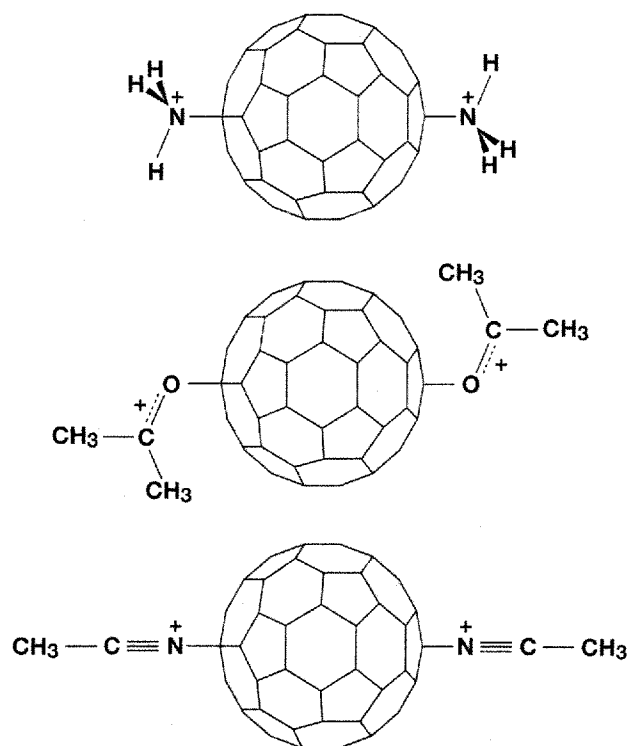
Fig. 2. Shows cage structure for C_{60} fullerenes as described in the review article by Bohme (1992). (Three examples of proposed "winged" structures for double adducts of the type $C_{60}(XH)_2^{2+}$ where $XH=NH_3,(CH_3)_2CO$,and CH_3CN.

1991) and are found to be the end product of forest fires (Richter and Howard, 2000; Calcote et al., 1990; Frencklach, 2002). The main difference between fullerenes and PAHs is that the former has no hydrogen (C_{60}), while PAHs have hydrogen ($C_{2n}H_x$).

There is a "zipper" mechanism often discussed with regard to the formation of fullerenes. Hunter et al. (1994) gave one explanation on how this "zipper" mechanism works. They based their conclusions on laboratory measurements where they used a laser vaporization of graphite source which produced ionized carbon chains and rings. The cluster ions of carbon were injected at different energies into a Helium buffer gas where they were thermalized. They use a quadrupole mass spectrometer to select cluster ion products of different mass. Their measurements showed that fullerenes were produced from intermediate mono-cyclic, bicyclic and tricyclic (i.e., polycyclic) carbon rings. Then from low frequency vibration modes and strain relief of the larger cyclic rings and the resulting spiraling of polyyne chains, fullerenes form. These measurements also showed that the activation energy ~ 2.4 eV for fullerene formation were unexpectedly low. In the papers by Thaddeus (1994, 1995) the argument is made that PAHs are not likely to be the dominant path to heavy molecules or aerosols and grains within diffuse molecular clouds, but rather fullerenes which have their origins from long carbon chains which then fold into polycyclic rings and then fullerenes. Thaddeus (1994, 1995) then go on to say that fullerenes from C^+ insertion reactions with H, O, N, S, etc, can then grow into larger "amorphous carbon" organic polymers. There is experimental evidence of clustering of fullerenes (C_{60})$_n$ with $n < 147$ observed in the laboratory by Martin et al. (1996) with major peaks in their mass spectrum at $n = 13$ and 55. Whether such clustering within Titan's atmosphere can occur must await further laboratory measurements more characteristic of Titan's atmosphere.

If heavy negative ions observed by Cassini are fullerenes, then they should prefer a negative charge. Laboratory measurements by Yang et al. (1987), Wang et al. (1991) and Wang et al. (2005) have shown C_{60} to have high electron affinity (2.6–2.9 eV), and since electron attachment for PAHs occur for electron affinities > 1 eV (Moustefaoui et al., 1998), fullerene negative ions are allowed. But, in some cases fullerenes can be stripped of electrons to form +1 and +2 cations (Weiske et al., 1991). The measurements by Moustefaoui et al. (1998) were made at relatively high electron temperatures ~300 K or more and that it is difficult to achieve lower electron temperatures T~150 K in the laboratory (Goulay et al., 2004). Titan's upper atmosphere and ionosphere are relatively cold with neutral and ion temperatures ~150 K (Waite et al., 2005, 2007), but the electron temperatures can be quite hot with thermal electron temperatures $T_{e,c}$~1000 K (Wahlund et al., 2005) and hot component photoelectron temperatures $T_{e,h}$~20,000 K (Hartle et al., 2006a,b; Coates, 2009a; Cravens et al., 2009). It is important to note that electron attachment to fullerenes C_{60} and C_{70} has an exponential temperature dependence that increases rapidly for $T_e > 500$ K with relatively high rate coefficient β_e~3×10^{-8} cm^3/s (Smith et al., 1993; Spanel and Smith, 1994; Spanal and Smith, 1995; Jaffke et al., 1994) at T_{ec}~1000 K (Wahlund et al., 2005), so electron attachment to fullerenes seems allowed. More recently, Ågren et al. (2009) did a more systematic study of Titan's ionosphere and determined the dayside peak densities to be 2500–3500 el/cm^3 and the nightside peak densities to be 400–1000 el/cm^3. The ionospheric peak electron temperature is rather constant near 350–700 K. The lower electron temperatures given in this report will give lower electron attachment rates for C_{60}~10^{-8} cm^3/s and for electron densities N_{ec}~3000 el/cm^3 on the dayside attachment time scales are ~9 h, while for nightside with N_{ec}~1000 el/cm^3 electron attachment time scales ~27 h. If one uses the temperature for photoelectrons with T_{eh}~20,000 K and N_{eh}~10 el/cm^3 (Hartle et al., 2006b for TA) the fullerene attachment rate is estimated to be β_{eh}~4.4×10^{-7} cm^3/s with attachment time scales τ_{eh}~$1/(N_{eh}\beta_{eh})$ ~2.6 days which are longer than the thermal electron attachment time scales.

In case of positive ions recombination time scales are α~$10^{-5}/T_{ec}^{0.6}$~2×10^{-7} cm^3/s for T_{ec}~700 K are relatively fast $\tau_{\alpha e}$~1–2 h (Cravens et al., 2006). Photoionization rates for atoms and smaller molecules, for which the ionization potentials are ≥ 10 eV, are typically ~10^8 s (see Sittler et al., 2008) or time scales ~3 yr. Borucki et al. (2006) considered photoemission rates for embryo aerosols (3 Å) within Titan's lower atmosphere for heights less than 400 km. Fullerene sizes are similar to the embryo aerosols considered by Borucki et al. (2006) and have ionization potentials ~7.07 eV (Bettens and Herbst, 1995), so photoemission rates for fullerenes and their clusters are expected to be higher than those for atomic and molecular ions. Their calculations do show that when in shadow photo-detachment of electrons from negative ions (i.e., fullerenes) will be much lower and thus more likely to retain their negative charge. This is supported by the CAPS-ELS observations reported by Coates et al. (2009b) where heavy negative ions are more important near terminator local times at Titan. Estimation of the actual charge state of fullerenes requires development of a complex model similar to that by Borucki et al. (2006), including photo-detachment rates, ion–neutral and ion–ion charge transfer rates and is thus beyond the scope of this paper. But, the relatively high electron affinities and electron attachment rates are consistent with negative charge states for fullerenes. This will be the subject of future work.

Ionization of the upper atmosphere comes in part from solar UV, magnetospheric electrons and X-ray photons but also arises from bombardment by hot keV magnetospheric heavy oxygen ions (Hartle et al., 2006a,b,c) and energetic protons and oxygen ions (Mitchell et al., 2005 and Cravens et al., 2008). The energetic protons and > 10 keV oxygen ions can penetrate below 950 km (Luna et al., 2003; Cravens et al., 2008; Hartle et al., 2006c) where the heavy positive and negative ions are observed by Cassini (Coates et al., 2007; Waite et al., 2007). Galactic cosmic ray protons (Capone et al., 1983; Molina-Cuberos et al., 1999) penetrate much more deeply and dominate ionization in the lower atmosphere. Ionization layers at altitudes ~700 km can form due to meteoritic dust impacts as shown by Molina-Cuberos et al. (2001). Ionization layers ~500 km were observed by the Cassini radio science experiment by Kliore et al. (2008). The key to the formation of fullerenes and PAHs within this environment is then the combination of relatively high methane abundance and the high-energy radiation input to the atmosphere.

2.3. Role of oxygen input from magnetosphere and micrometeorites

The role of oxygen becomes particularly significant for astrobiology if fullerene formation occurs. Oxygen is an important ingredient of amino acids and other chemical compounds necessary for evolution of life, and exothermic oxidation of nutrients is critical to biochemical processes. Major abundance of free oxygen in Titan's highly reducing atmosphere is highly unlikely (Raulin and Owen, 2003), but the bound molecular form is found in trace species such as CO at the 60 ppm level in Titan's atmosphere as discovered by Lutz et al. (1983). This was later followed by the discovery of CO_2 in Titan's atmosphere at the 1.5 ppb level by Samuelson et al. (1983), who showed that water entry from above may be required in order to explain the presence CO_2 having a relatively short lifetime ~5×10^4 yr. In both cases the oxygen is locked up in the CO and CO_2 which are fairly stable molecules ($CO \rightarrow C+O+11.17$ eV; $CO_2 \rightarrow CO+O+5.46$ eV; $CO_2 \rightarrow C+O+O+16.63$ eV). It was argued that the CO was probably primordial in origin but the recent model results by Hörst et al. (2008) showed that this was not required due to the entry of keV oxygen ions to Titan's upper atmosphere (Hartle et al., 2006a,b).

Oxygen can be introduced into Titan's upper atmosphere by entry and ablation of micrometeorites containing water molecules (Samuelson et al., 1983). Models of Titan's atmosphere after the discoveries of CO and CO_2 required an inward flux of oxygen as summarized in Table 1. In the case of Yung et al. (1984) they required oxygen influx ~6.1×10^5 O atoms/cm^2/s, while that by Toublanc et al. (1995) used a downward flux ~1.5×10^6 O atoms/cm^2/s. The mechanism of meteoroid ablation in Titan's upper atmosphere was initially suggested by Ip (1990) for the case of water ice particles and stony particles. Then English et al. (1996) proposed a micrometeorite ablation model for water

Table 1
Summary of oxygen source for Titan's upper atmosphere.

	Oxygen source	In flux rate (O/cm^2/s)
Lutz et al. (1983)	CO discovery ~60 ppm	
Samuelson et al. (1983)	CO_2 discovery ~1.5 ppb @ 110 mbars E ring & Meteoricand meteoric dust as source of O	6.1×10^5
Yung et al. (1984)	Based on CO &and CO_2 chemistry	6.1×10^5
Toublanc et al. (1995)	Chemical model with CO &and CO_2	1.5×10^6
English et al. (1996)	Micrometeorite dust ablation	3×10^6
Lara et al. (1996)	CO &and CO_2 model based on English et al. (1996)	3×10^6
Coustenis et al. (1998)	Discovery of H_2O ~8 ppb @ 400 km	0.8–2.8×10^6
Hartle et al. (2006a)	Ta keV magnetospheric O^+	1.8×10^6
Hartle et al. (2006b)	Ta keV magnetospheric O^+	1.1×10^6

entry with peak deposition rate at ~700 km altitude. Their model showed peak flux ~3×10^6 mol/cm^2/s. The discovery of water in Titan's atmosphere by Coustenis et al. (1998) with mole fraction ~8 ppb at 400 km altitude ended any doubts about the presence of water products in Titan's upper atmosphere. The Coustenis et al. (1998) results inferred an influx rate of 0.8–2.8×10^6 mol/cm^2/s.

Cassini results continue to build the case for oxygen and water sources in the upper atmosphere. Hartle et al. (2006a,b) presented the first observational evidence of magnetospheric keV oxygen ions into Titan's upper atmosphere with an estimated influx rate ~1.1×10^6 O atoms/cm^2/s at the exobase. The presence of negative oxygen ions in Titan's upper atmosphere can be inferred by the mass 16 peak in Fig. 1 from T16 adapted from Coates et al. (2007). This might be expected due to the high electro negativity of oxygen atoms. This is also suggested by Cravens et al. (2008), although Vuitton et al. (2009b) based on T40 heavy negative ion measurements argue against a significant presence of O$^-$. When Vuitton et al. (2009b) included the influx of oxygen ~10^5 O/cm^2/s, which is 5% of "typical" of that reported by Cravens et al. (2008) for T5 and 10% of that reported by Hartle et al. (2006a,b) ~10^6 O/cm^2/s for TA, the O$^-$ densities increased from a maximum of 10^{-6} O$^-$/cm^3 at 1100 km altitude to 4×10^{-3} O$^-$/cm^3 at 1100 km. If a more typical value of the influx is used and the uncertainties in the cross-sections are accounted for one could argue that elimination of O$^-$ from the CAPS-ELS mass spectrum cannot yet be made. It is also important to note that there are times when no heavy ions are present in the upstream magnetospheric flow and times when it dominates the upstream flow (Sittler et al., 2009) and therefore one must consider such complications when interpreting negative ion mass spectra for specific Titan flybys (i.e., T16 vs. T40).

The CDA observations of E-ring dust particles by Srama et al. (2006) within Saturn's outer magnetosphere allows one to estimate an influx rate of water molecules into Titan's upper atmosphere ~2.5×10^5 water mol/cm^2/s at the exobase. In the case of magnetospheric oxygen ions and E-ring dust particles, the source of the water and oxygen can be traced back to Enceladus (Johnson et al., 2005; Sittler et al., 2006).

2.4. Trapping of free oxygen and hydroxyl ions in seed particles

Laboratory experiments show that C$_{60}^+$ 6–16 keV ions (lab frame kinetic energy) can trap lower mass target gas atoms inside the fullerenes. Magnetospheric keV O$^+$ ions incident upon Titan's upper atmosphere can be implanted and become trapped within Titan's fullerenes. The laboratory measurements are quite extensive for fullerene trapping of target noble gases such as He, Ne, Ar, Xe and Kr. Weiske et al. (1991) found that C$_{60}$+He → C$_x$He ($46 < x < 60$) for He target gas at C$_{60}^+$ incident energy (product fractional percentage) of 6 keV (30%), 8 keV (34%), 10 keV (14%) and 16 keV ($< 1\%$). The equivalent center of mass energies for incident He ions would be 33, 44, 56 and 89 eV, respectively. For incident O$^+$ ions the equivalent center of mass energy would range from 132 to 356 eV. As keV O$^+$ ions lose energy within Titan's upper atmosphere (e.g., Shah et al., 2009) and their energies drop below 400 eV they can become trapped in fullerenes with higher probability. This trapping will occur deeper in the atmosphere as the O$^+$ incident energy increases (i.e., ion penetration into atmosphere increases as the ion initital energy increases). In case of Argon center of mass energies used were ~450 eV, while for Kr center of mass energies were ~1230 eV (Caldwell et al., 1991, 1992). The higher center of mass energies can cause fragmentation of the fullerene with ejection of carbon atoms. Higher center of mass collisions up to 1 keV for O$^+$ have yet to be done. In some cases more than one He atom was implanted into a fullerene.

Caldwell et al. (1991, 1992) did similar experiments using He, Ne and Ar and found end products C$_{60}$He$^+$, C$_{60}$He$_2^+$, C$_{70}$He$^+$, C$_{84}$He$^+$, C$_{55}$Ne$^+$ and C$_{55}$Ar$^+$. Xe and Kr were not captured due to their larger size as compared to the space inside fullerenes. These results are consistent with X-ray crystallography measurements of fullerene dimensions and size within their hollow cage.

From these laboratory results two mechanisms are invoked. Mechanism 1 is the "low pressure limit" for which the ion is injected directly into the fullerene, while mechanism 2 is in the "high pressure limit" for a collision induced fracture of the carbon cage occurring first and then being followed by atom capture as an ion complex. The first mechanism could apply at Titan for direct injection of oxygen ion into the fullerene. Although, most of the oxygen ions will form CO and CO$_2$ once thermalized, the direct implantation mechanism does not have this problem. The capture cross-section (fullerene geometric cross-section $\sigma_F \sim \pi r_F^2 \sim 4 \times 10^{-15}$ cm^2) is quite large. Results of Coates et al. (2007) for mean negative ion mass ~4000 amu (i.e., embryo aerosol) give 4000/720–6 cages, radius $r_A \sim 7$ Å or larger and geometric cross-section $\sigma_A \sim \pi r_A^2 \sim 1.5 \times 10^{-14}$ cm^2.

Trapping of oxygen ions inside the fullerenes provides a stable means of oxygen conveyance within the upper atmosphere which is ultimately delivered to the surface. Complex chemistry of pre-biotic and even biotic interest could occur as oxygen-laden aerosol particulates precipitate to any surface hot spots associated with local cryovolcanism (Sotin et al., 2005; Lopes et al., 2007; Nelson et al., 2008) and where liquid water might be present near the surface.

In the modeling by Michael and Johnson (2005) and Michael et al. (2005), the energy input into Titan's upper atmosphere by keV magnetospheric heavy ions, the heavy ions tended to dominate the energy input to Titan's upper atmosphere. They assumed the ions were directed down into Titan's atmosphere. This was the case since for V1 the convective electric field pointed radially away from Saturn so that pickup ions on the Saturn side of Titan would be accelerated into Titan's upper atmosphere. For T5 the electric field is pointed southward so pickup ions are accelerated into Titan's northern hemisphere. In cases when Titan is above the magnetospheric current sheet the pickup ions will be accelerated into Titan's southern hemisphere. They found the pickup ions tended to dominate the energy input to Titan's upper atmosphere relative to the magnetospheric input. Therefore, implantation of N$^+$, N$_2^+$ and CH$_4^+$ pickup ions into the fullerenes could also be occurring at levels comparable to oxygen input rates.

2.5. Transport to lower atmosphere and surface as aerosols

Estimates of the mass flux of the heavy ions observed in Titan's ionosphere downward to the surface can address whether these ions might account for the aerosols observed by Tomasko et al. (2005) using the Huygens DISR imaging system. In principle we can also estimate the potential surface delivery rate of oxygen bound in fullerenes due to aerosol transport. As stated earlier the heavy negative ion density increased with depth in the atmosphere with the highest masses and number densities at the minimum altitude 950 km probed by Cassini (Coates et al., 2007). Such increases likely continue to lower altitudes and perhaps ultimately to maximum densities of aerosol cloud layers 100–200 km or lower (de Kok et al., 2007) above the surface. Lavvas et al. (2008a,b) developed a photochemical model of Titan's atmosphere which extended from the surface to the upper atmosphere $z \sim 1400$ km altitude. In these papers the size distribution of the haze particles was derived with height using a 1D diffusive transport code with source and sink terms for the size distribution of particles. The calculations determined the size

distribution of the aerosols at different heights with peak number densities $\sim$100 part/cm^3 and size $r_A \sim 10^{-3}$ μm at 950 km. Lavvas et al. (2008b) give particle mass $\sim$5000 amu, very close to that observed by Coates et al. (2007) at 950 km. Near the surface these latter authors estimate particles sizes $\sim$0.5 μm with number densities $\sim$7 part/cm^3.

Borucki and Whitten (2008) and built on earlier models by Borucki et al. (1987, 2006), modeled haze particle distributions for heights less than 150 km. They assumed three mass fluxes 4×10^{-14} kg/m^2/s for case B, 4×10^{-13} kg/m^2/s for case C, and 10^{-12} kg/m^2/s for case D, also assume mass flux conservation, and do not use diffusion terms which are essentially unknown. Using Stokes Equation from Roe et al. (2002), they estimated fall velocity $\sim$5 $\times 10^{-6}$ m/s for case B and $\sim$4 $\times 10^{-5}$ m/s for case D. The particle sizes were $r \sim$0.45 μm for case B, 0.95 μm for case C and $r \sim$1.3 μm for case D. The particle abundances were $\sim$6 $\times 10^6$ part/m$^3 \sim$6 part/cm^3, which are very close to that estimated by Lavvas et al. (2008b). In this paper we estimate a simplified fall velocity applicable to the higher altitudes probed by Cassini which includes simple frictional drag from molecular collisions on the heavy ions. The expression is as follows:

$$V_{\text{drift}} = \frac{M_{\text{seed}} g(z)}{N_{N_2} M_{N_2} w_{N_2} \sigma_{\text{seed}}} \tag{1}$$

with

$$\sigma_{\text{seed},j} = \pi r_{\text{seed},j}^2 \tag{2}$$

where M_{seed} is the mass of the heavy ion observed by Coates et al. (2007) and we refer to as seed particles for the aerosols (or embryo aerosols), $g(z)$ is the local acceleration of gravity which is a function of height z, N_{N_2} is the number density of N$_2$ molecules, $M_{N_2} = 28$ amu is the mass of N$_2$, w_{N_2} is the thermal speed of the N$_2$ molecules and σ_{seed} is the geometric cross-section of the seed particles plus that of the N$_2$ molecules. We use this expression to estimate the heavy ion fall speed at 950 km which one finds to be $\sim$10 m/s for fullerenes and $\sim$0.4 m/s for PAHs (i.e., both with same M/Q, see previous discussions about ion charge state and cross-sectional size).

Negative Ion Fall Velocity
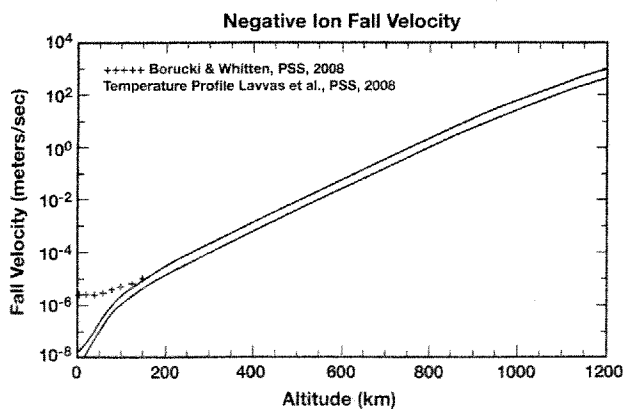
Fig. 3. Plot of aerosol fall velocity (m/s) versus altitude based on our simplified expression in Eqs. (1) and (2) from above 950 km down to the surface. Two curves are shown for particles mass 4000 and 40,000 amu (top curve). If particles are spherical they will fall faster as they grow, but if more planar then their fall velocity is independent of particle mass for a given height. We also show the estimates by Borucki and Whitten (2008a,b) for altitudes < 150 km. Our estimate is less than Borucki and Whitten (2008a,b) as would be expected, since the particle size $\sim$1 μm is $\gg$6.5 Å (4000 amu) and 14 Å (40,000 amu) for seed particles observed above 950 km altitude. Our expression for spherical 1 μm sized particles would yield fall velocities several orders of magnitudes greater than that shown here for 40,000 amu particles.

We show in Fig. 3 the fall speed of the haze particles as a function of height for different assumed haze particles mass (4000 and 40,000 amu). In reality, as the haze particles fall they will grow in size and tend to fall faster as they become more massive except for the increase in frictional drag due to the increased cross-sections and atmospheric N$_2$ density with depth. Looking at Eqs. (1) and (2), heavier spherical ions will fall faster linearly with particle radius r (i.e., $M_P \sim (4\pi/3)\rho r^3$ and $\sigma_P \sim \pi r^2$). Fluffy or planar particles will fall at a speed independent of particle mass at a given height. Assuming fullerenes as the primary aerosol component, and taking the ion number densities with mean mass $\sim$4000 amu of the heavy negative ions we estimate at 950 km altitude a downward mass flux $\Phi \sim 2.7 \times 10^{-14}$ kg/m^2/s. This flux is smaller than the lower limit $\Phi \sim 4 \times 10^{-14}$ kg/m^2/s used by Borucki and Whitten (2008a,b) and constrained by Tomasko et al.'s (2005) aerosol observations but considering uncertainties identical. If the mass density flux increases below 950 km as expected, then the heavy ions observed above 950 km may be sufficient to account for all the aerosols observed by Tomasko et al. (2005) near the surface. If one uses the mass flux rate $\sim$4 $\times 10^{-14}$ kg/m^2/s and a surface mass density $\sim$420 kg/m^3 it will take $\sim$300 Myrs to accumulate an aerosol depth of one meter (420 kg/m^2) uniformly distributed around the globe. If one uses the higher mass fluxes of Borucki and Whitten (2008a,b) the accumulation times could be as short as $\sim$10 Myrs.

2.6. Loss of ionospheric ions to Titan's surface

We now consider the effect of heavy negative ion drift and formation of an ambipolar electric field. We have ignored the role of heavy positive ions $N_{\text{Heavy},j}$ since they are less abundant than the dominant ionospheric ions $N_{\text{ION},j}$. Then assuming the seed particles are negative and imposing the charge neutrality condition

$$\sum_j N_{\text{seed},j} Q_{\text{seed},j} + N_e = \sum_j N_{\text{ION},j} + \sum N_{\text{Heavy},j} Q_{\text{Heavy},j} \tag{3}$$

$$N_e \cong \sum_j N_{\text{ION},j} \tag{4}$$

for which the heavy negative ions $\sum_j N_{\text{seed},j} Q_{\text{seed},j} \ll N_e$, impose zero current condition

$$e \sum_j N_{\text{seed},j} Q_{\text{seed},j} V_{\text{drift,seed},j} - e \sum_i N_{\text{iono},i} V_{\text{drift,iono},i} = 0 \tag{5}$$

(the electrons are assumed to be collisionally coupled to the neutral atmosphere) and frictional drag one can derive the following expression for the ambipolar electric field

$$E(z) = \frac{M_{N_2} g(z)[N_{\text{seed}} Q_{\text{seed}}(M_{\text{seed}}/M_{N_2}) - N_{\text{ION}}(\sigma_{\text{seed}}/\sigma_S)]}{e[N_{\text{seed}} Q_{\text{seed}}^2 + N_{\text{ION}}(\sigma_{\text{seed}}/\sigma_S)]} \tag{6}$$

The following parameters are used $\sigma_{\text{seed}}/\sigma_S \sim$40 (typical elastic scattering cross-section is $\sigma_S = 5 \times 10^{-15}$ cm^2 for ion–neutral collisions), $N_{\text{ION}} = 5000$ ions/cm^3 (HCNH$^+$ ion), $N_{\text{seed}} = 200$ anions/cm^3, $M_{\text{seed}}/M_{\text{ION}} \sim$143 ($M_{\text{seed}} = 4000$ amu), seed particle charge state $Q_{\text{seed}} = 1$, $E(z) = 0.180$ μV/m, $a_{\text{seed}} = eE(z)/M_{\text{seed}} \sim$0.43 cm/s$^2 \ll g(z) = 72$ cm/s^2 at 950 km, $a_{\text{ION}} = eE(z)/M_{\text{ION}} \sim$62 cm/s$^2 \sim g(z)$ at 950 km, and then with $V_{\text{drift seed}} \sim$10 m/s and $V_{\text{drift iono}} \sim$0.4 m/s. Using these we estimate a loss of positive ionospheric ions to the lower atmosphere by negative ions dragging them along $\sim$2 $\times 10^5$ ions/cm^2/s (i.e., at lower altitudes they probably recombine and become part of the lower atmosphere). If, electrons were free to move vertically, they would tend to short circuit this electric field. The net effect would be to reduce the downward drag on the ionospheric ions by the heavier negative ions. This loss is not very large, and about 4% of the ionospheric wind loss from the topside ionosphere (Hartle et al.,

2008; Sittler et al., 2009). The atmospheric loss from the fall of negative ions in units of mass 28 is much larger: $\sim 5 \times 10^6$ ions/cm^2/s and when one combines the two losses the total ion loss $\sim 5.2 \times 10^6$ ions/cm^2/s. This translates to a loss rate of 2.4×10^{-16} gm/cm^2/s and can be compared to a loss rate $\sim 5 \times 10^{-16}$ gm/cm^2/s at 1000 km altitude estimated independently by Wahlund et al. (2009).

2.7. Other observations and final comments

2.7.1. Fullerenes versus PAHs

We first address the issue of fullerenes versus PAHs with the former composed only of carbon C_n, while PAHs are composed of both carbon and hydrogen C_nH_m. Hydrocarbons like C_2H_2 are considered unsaturated in hydrogen, while C_2H_6 is considered saturated. It is sometimes implied that since Titan's atmosphere is rich in hydrocarbons with relatively large amounts of hydrogen, that hydrogen poor species such as fullerenes would not form. But, in fact the reverse may be true and many experts in the study of ISM such as Thaddeus (1994, 1995) favored fullerenes over PAHs in an environment similar to that for Titan (i.e., low temperatures $T < 150$ K). Observation of negative ions in the interstellar medium were primarily composed of polyyne radicals $C_{2n}H^-$ (McCarthy et al., 2006; Brünken et al., 2007; Sakai et al., 2007; Remijan et al., 2007) or unsaturated carbon nitrogen species such as C_3N^- (Thaddeus et al., 2008). Vuitton et al. (2007) and later Vuitton et al. (2009b) showed significant abundances of polyynes (C_2H_2, C_4H_2, C_6H_2, C_8H_2) in Titan's atmosphere at 1100 km using a photochemical model constrained by INMS ion measurements. In Vuitton et al. (2007) they also note that the abundance for the higher carbon chain polyynes within Titan's atmosphere did not decrease as fast as that in other photochemical models (Yung et al., 1984; Toublanc et al., 1995; Wilson and Atreya, 2004), the ISM (MacLeod et al., 1984; Remijan et al., 2006; Cernicharo et al., 2001) and/or laboratory measurements (Coll et al., 1999) as the number of carbon atoms increased in the carbon chain. It is also well known, as discussed in Thaddeus (1994, 1995) and Vuitton et al. (2007), that unsaturated polyynes can polymerize into long carbon linear chains from which fullerenes can form (Hunter, 1994; Thaddeus, 1994, 1995). As discussed in Vuitton et al. (2007) with photodissociation making the polyyne radical $C_{2n}H_2 + h\nu \rightarrow C_{2n}H + H$ which can then react with another polyyne $C_{2n}H + C_{2m}H_2 \rightarrow C_{2(n+m)}H_2 + H$ to make a longer carbon chain, so very long carbon chains with very small amounts of H can form in Titan's atmosphere. The above reactions have been confirmed both experimentally and theoretically (Smith and Rowe, 2000; Smith et al., 2006; Berteloite et al., 2008). Laboratory measurements have also shown fullerenes can form large clusters $(C_{60})_n$ with index n as high as $n \sim 146$ (Martin et al., 1996).

This does not mean to say that PAHs cannot also form in Titan's atmosphere since the aromatic benzene C_6H_6 and its radical phenyl C_6H_5 are present in Titan's atmosphere (Vuitton et al., 2009a) and similar polymerization reaction paths may occur to make PAHs (Waite et al., 2007; Vuitton et al., 2007). As we have stated previously both processes could very well be occurring at the same time and heavier aerosols could be mixtures or conglomerations of fullerenes and PAHs (see comments by Thaddeus, 1994, 1995 on large aerosol formation).

2.8. Comment on UVIS observations of aerosols

With regard to the UVIS observations by Liang et al. (2007) there could be a charge neutrality problem. Using Cassini UVIS stellar occultation data, Liang et al. (2007) observed the haze layer down to 400 km altitude. Assuming a scattering radius $r_A \sim 12.5$ nm for aerosols, they estimated a "tholin" particle density $\sim 10^4$ part/cm^3 at 950 km and $\sim 10^6$ part/cm^3 at 400 km altitude. Such particle sizes could be in agreement with the Coates et al. (2007) heavy negative ion results if the particles are flat PAHs with radii $r_{seed} < 6$ nm. Since Liang et al.'s (2007) results are not very sensitive to particle size, UVIS could also be seeing ~ 6 nm size or even smaller particles. The large number of "tholin" particles observed by UVIS at 950 km $\sim 10^4$ part/cm^3 is much greater than that observed by Coates et al. (2007) for negative ions and Waite et al. (2007) for heavy positive ions.

If a significant fraction of the haze particles observed by UVIS are charged, then we have a conflict and charge neutrality would become a serious problem when the Langmuir Probe data is also considered for which $N_{ec} < 5000$ el/cm^3 (Wahlund, private communication, 2009). If Coates et al. (2007) are really seeing fullerenes then they may be too small ($r_A < 12$ Å) for UVIS to detect and Liang et al. (2007) are seeing particles too big to be observed by CAPS-ELS. But this would not resolve the charge neutrality problem unless all the haze particles observed by UVIS are not charged. For lower mass negative ions, as modeled by Vuitton et al. (2009b) and also found in ISM the ratio $C_{2n}H^-/C_{2n}H \ll 1$, this ratio tends to increase with increase in the number of carbon atoms per carbon chain. Liang et al.'s (2007) results do show that the haze particles have a similar scale height to acetylene, which one might expect if the acetylene is the source of the "tholin" particles. Acetylene can polymerize and make fullerenes while benzene is probably needed to make PAHs. This would favor more fullerenes relative to PAHs.

2.9. Entrapped oxygen in aerosols

Using the influx rate of O^+ keV of 1.1×10^6 O/cm^2/s from Hartle et al. (2006b), a seed cross-section $\sigma_{seed} \sim 4.5 \times 10^{-14}$ cm^2 and $N_{seed} \sim 200$ ions/cm^3 an implantation rate $\sim 10^{-5}$ O implanted seed/cm^3/s. The atmospheric volume needed to make one of the aerosols observed by Tomasko et al. (2005) is $\Delta V_{ionosphere} \sim 1.9 \times 10^6$ cm^3, so there are ~ 19 O atoms/s implanted within each aerosol grain. If the seed particle fall rate is ~ 3 m/s and one uses a column density ~ 100 km for O^+ penetration, we estimate $\sim 6.3 \times 10^5$ O/aerosol. One can then estimate $\sim 2 \times 10^9$ fullerenes per aerosol, so that there are $\sim 0.05\%$ of the fullerenes with oxygen atoms. If one uses the medium mass flux limit by Borucki and Whitten (2008a,b) $\Phi \sim 4 \times 10^{-13}$ kg/m^2/s for the lower atmosphere one gets $\sim 6.8\%$ of the aerosols being in the form of fullerenes. But, these are lower limits since the heavy negative ion densities and masses are expected to increase below 950 km.

The estimated mass flux of free oxygen to the surface is then 0.1% of that incident onto the upper atmosphere from the magnetosphere, the bulk of the oxygen going to formation of CO and CO_2.

Based on the above values for aerosol mass flux to the surface, the aerosol mass fraction from fullerenes, and fractional upper atmospheric oxygenation of the fullerenes, we estimate an oxygen mass flux to the surface of 3×10^{-3} kg/m^2 per 300 Myr. This amounts to 7×10^{-6} mass fraction of the one-meter aerosol layer accumulated in 300 Myr. In the same accumulation time, abiotic atmospheric oxygen production condensed to the surface on Earth, mostly from UV photolysis of atmospheric water vapor is 130 kg/m^2 (Chyba and Hand, 2001). For comparison, the mass fraction of photosynthetic oxygen in terrestrial sea water is 10^{-5} (Schlesinger, 1997).

2.10. Heavy ions and haze generation with oxygen model

Fig. 4 summarizes the "heavy ions and haze generation with oxygen model" as presented in this paper. The top layer signifies Saturn's magnetosphere with the exobase forming its lower
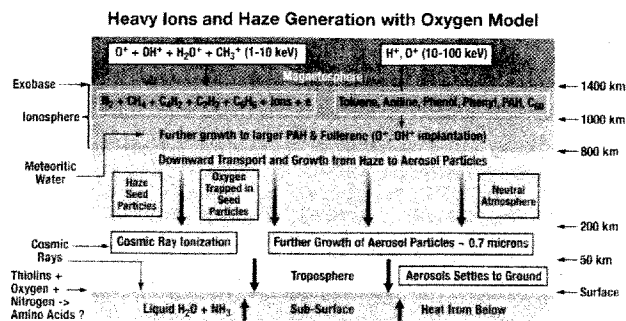
Fig. 4. Summary slide shows our "heavy ion and haze generation with oxygen model". See text for details.

boundary. The ion composition of water group ions, methane group ions with energy 1–10 keV and more energetic H^+, O^+ ions (10–100 keV). Below the exobase lies the topside ionosphere, with lower ionosphere between 800 and 1400 km, where the keV oxygen ions can become trapped with fullerenes growing along with the PAH population. Cravens et al. (2008) show that the keV O^+ ions deposit a significant fraction of their energy below 950 km altitude.

We also show cosmic rays penetrating to the lower atmosphere and meteoritic dust down to lower ionosphere. Below 950 km we assume further grain growth in size which then continues down to ~400 km. Below 200 km further growth presumably occurs at depths of maximum energy deposition from ionization by primary and secondary cosmic ray shower particles. In addition to grain growth, the cosmic rays can provide radiogenic energy to the aerosols which can then free the oxygen within the aerosols and possibly drive pre-biotic chemistry within the grains. Even after precipitation to the surface, the precipitating aerosol grains would continue to be processed chemically by irradiation from cosmic ray showers, also producing oxygen in surface or buried water ice to many meters in depth. Although height integrated cosmic ray ion production rates above 50 km maybe 100 times greater than that below 50 km (see Capone et al., 1983; Molina-Cuberos et al., 1999), the time scales for descending aerosols ~100–1000 yr are much shorter than the surface irradiation times scales ~30–300 Mys (i.e., time it takes to accumulate ~1 m of aerosols to surface). The descending aerosols may have a larger surface area for exposure than that on the surface. Therefore, cosmic rays will be effective in driving the aerosol chemistry at all phases of their time history from formation at the highest altitudes ~950 km down to the surface.

Borucki et al. (2006) presented evidence for ion clusters such as $CH_5^+CH_4$, $C_7H_7^+$, $C_4H_7^+$ and $H_4C_7N^+$ to form below 400 km due to the ionization of nitrogen and methane by cosmic rays. They show that PAHs, which can be electrophilic (see Bakes et al., 2002), can form negative ions and significantly reduce electron densities, between 150 and 350 km, below that one would otherwise expect. In addition to PAHs fullerenes are also highly electrophilic as discussed previously and will similarly form negative ions. They also show that three-body electron-ion recombination collision will further reduce electron densities below expectations for heights <60 km (Huygens HASI conductivity probe measurements require low electron densities as discussed in Borucki and Whitten, 2008a,b). Borucki et al. (2006) also suggest that one must consider very small aerosols called embryos which can easily be ionized and can only retain charge states Q~1. These particles are similar in size to that observed above 950 km as heavy negative ions by Coates et al. (2007). Aerosol charging can contribute to atmospheric conductivities which can then be measured by the Huygens HASI instrument (see Fulchignoni

et al., 2005). The haze particles then fall through the troposphere to the surface. At the surface, due to accumulation of aerosol particles we show a mixture of "tholins", oxygen, nitrogen and amino acids with the latter a speculation.

Below the surface a liquid ocean has recently been detected (Lorenz et al., 2008; Stiles et al., 2009) where interior models (Tobie et al., 2005) require ammonia as an anti-freeze since model temperatures are too low to allow pure liquid water to occur below the surface. It has been suggested that methanogenic life with this liquid ocean could be the source of Titan's methane which has a lifetime less than 100 Myrs (Fortes, 2000; McKay and Smith, 2005). This liquid water and heat, via the cryovolcanism that may have been observed (see Lopes et al., 2007; Neish et al., 2006), can then allow exobiological processes occur, especially if free oxygen is present. The observation of lakes by Cassini radar (Stofan et al., 2007), presents another tantalizing possibility for exobiological processes occurring at Titan. Recently, the Cassini VIMS experiment by Brown et al. (2008) has shown that these lakes contain ethane and are thus probably a mixture of organic molecules (see Raulin, 2008). If the aerosols discussed here do contain oxygen and land on these organic lakes a unique environment with significant astrobiological potential is created.

How important could the magnetospheric oxygen be to the astrobiological chemistry of the Titan surface and liquid subsurface environments? Over 300 Myr we estimate an accumulated fractional mass column density of $5–6 \times 10^{-7}$ of oxygen in a one-meter aerosol layer. This ratio would presumably remain representative of the exogenic material over time as this layer is mixed deeper into the regolith by geologic and impact processes. For comparison, the mass ratio of dissolved oxygen to water is 10^{-5} in terrestrial sea water. This is also near the upper limits of radiolytic surface production from jovian magnetospheric interaction with the surface of Europa for downward conveyance to its putative subsurface ocean (Cooper et al., 2001). By comparison, the exogenic oxygen at Titan is not significant at the macroscopic level for the bulk chemistry of the surface as compared to Earth and possibly Europa.

On the microscopic level the astrobiological significance might be much higher if purely organic aerosol grains acquired ice shells at the surface, e.g. through water frost deposition from Enceladus-like cryovolcanic activity. The free oxygen abundance would have sources both from magnetospheric oxygen injection into the fullerenes and from direct radiolytic production in the water ice in all atmospheric and surface phases. As noted above, nitrogen and methane ions could also be implanted within the grains plus their addition to the aerosols as they fall through Titan's atmosphere. Each Titan surface grain could be a microcosm of relatively abundant organics, water ice, and free oxygen trapped in fullerenes and the water ice. Heat from impacts and volcanic activity could then initiate the pre-biotic chemistry of life in microscopic versions of Darwin's warm ponds on Titan.

Acknowledgements

References

Ågren, K., Wahlund, J.-E., Gernier, P., Modolo, R., Cui, J., Galand, M., I. Müller-Wodarg, 2009. The ionospheric structure of Titan, Planet. Space Sci., in press, doi:10.1016/j.pss.2009.04.012.

Allamandola, L.J., Tielens, A.G.G.M., Barker, J.R., 1989. Interstellar polycyclic aromatic hydrocarbons: the infrared emission bands, the excitation/emission mechanism and the astrophysical implications. Astrophys. J. 71, 733–775.

Bakes, E.L.O., McKay, C.P., Bauschlicher, C.W., 2002. Photoelectric charging of submicron aerosols and macromolecules in the Titan haze. Icarus 157, 464–475.

Berteloite, C., Le Picard, S.D., Birza, P., Gzaeau, M.-C., Canosa, A., Bénilan, Y., Sims, I.R., 2008. Low temperature (39–298 K) kinetics study of the reactions of the C_4H radical with various hydrocarbons observed in Titan's atmosphere. Icarus 194, 746–757.

Bettens, R.P.A., Herbst, E., 1995. The interstellar gas phase production of highly complex hydrocarbons: construction of a model. Int. J. Mass Spectrom. Ion Processes 149/150, 321–343.

Bohme, D.K., 1992. PAH and Fullerene ions and ion/molecule reactions in interstellar and circumstellar chemistry. Chem. Rev. 92, 1487–1508.

Borucki, W.J., Levin, Z., Whitten, R.C., Keesee, R.G., Capone, L.A., Summers, A.L., Toon, O.B., Dubach, J., 1987. Predictions of the electrical conductivity and charging of the aerosols in Titan's atmosphere. Icarus 72, 604–622.

Borucki, W.J., Whitten, R.C., Bakes, E.L.O., Barth, E., Tripathi, S., 2006. Predictions of the electrical conductivities and charging of aerosols in Titan's atmosphere. Icarus 181, 527–544.

Borucki, W.J., Whitten, R.C., 2008. Influence of high abundances of aerosols on the electrical conductivity of the Titan atmosphere. Planet. Space Sci. 56, 19–26.

Bridge, H.S., et al., 1981. Plasma observations near Saturn: initial results from Voyager 1. Science 212, 217.

Broadfoot, A.L., et al., 1981. Extreme ultraviolet observations from Voyager 1-encounter with Saturn. Science 212, 206.

Brown, R.H., Soderblom, L.A., Soderblom, J.M., et al., 2008. The identification of liquid ethane in Titan's Ontario Lacus. Nature 454, 607–610.

Brünken, S., Gupta, H., Gottlieb, C.A., McCarthy, M.C., Thaddeus, P., 2007. Detection of the carbon chain negative ion C_8H^- in TMC-1. Astrophys. J. 664, L43–L46.

Calcote, H.F., Keil, D.G., 1990. Pure Appl. Chem. 62, 815.

Caldwell, K.A., Giblin, D.E., Hsu, C.S., Cox, D., Gross, M.L., 1991. Endohedral complexes of fullerene radical cations. J. Am. Chem. Soc. 113, 8519–8521.

Caldwell, K.A., Giblin, D.E., Gross, M.L., 1992. High energy collisions of fullerene radical cations with noble gases: capture of the target gas and charge stripping of C_{60}^+, C_{70}^+ and C_{84}^+. J. Am. Chem. Soc. 114, 3743–3756.

Capone, L.A., Dubach, J., Prasad, S.S., Whitten, R.C., 1983. Galactic cosmic rays and N_2 dissociation on Titan. Icarus 55, 73–82.

Cernicharo, J., Heras, A.M., Tielens, A.G.G.M., Pardo, J.R., Herpin, F., Guélin, M., Waters, L.B.F.M., 2001. Infrared Space Observatory's discovery of C4H2, C6H2, and benzene in CRL 618. Astrophys. J. 546, L123–L126.

Chyba, C.F., Hand, K.P., 2001. Life without photosynthesis. Science 292, 2026–2027.

Coates, A.J., Crary, F.J., Lewis, G.R., Young, D.T., Waite Jr., J.H., Sittler Jr., E.C., 2007. Discovery of heavy negative ions in Titan's ionosphere. Geophys. Res. Lett. 34, L22103, doi:10.1029/2007GL030978.

Coates, A.J., Wellbrock, A., Lewis, G.R., Jones, G.H., Young, D.T., Crary, F.J., Waite Jr., J.H., 2009b. Heavy negative ions in Titan's ionosphere: altitude and latitude dependence. Planet. Space Sci., in press, doi:10.1016/j.pss.2009.05.009.

Coates, A.J., 2009a. Interaction of Titan's ionosphere with Saturn's magnetosphere. Phil. Trans. R. Soc. A 367, 773–788.

Coll, P., Coscia, D., Smith, N., Gazeau, M.-C., Ramirez, S.I., Cernogora, G., Israel, G., Raulin, F., 1999. Experimental laboratory simulation of Titan's atmosphere: aerosols and gas phase. Planet. Space Sci. 47, 1331–1340.

Cooper, J.F., Johnson, R.E., Mauk, B.H., Garrett, H.B., Gehrels, N., 2001. Energetic ion and electron irradiation of the icy Galilean satellites. Icarus 149, 133–159.

Coustenis, A., Salama, A., Lellouch, E., Encrenaz, T., Bjoraker, G.L., Sameulson, R.E., de Graauw, T., Feuchtgruber, H., Kessler, M.F., 1998. Evidence for water vapor in Titan's atmosphere from ISO/SWS data. Astron. Astrophys. 336, L85–L89.

Cravens, T.E., Keller, C.N., Ray, B., 1997. Photochemical sources of non-thermal neutrals for the exosphere of Titan. Planet. Space Sci. 45 (8), 889–896.

Cravens, T.E., et al., 2006. Composition of Titan's ionosphere. Geophys. Res. Lett. 33, L07105.

Cravens, T.E., Robertson, I.P., Ledvina, S.A., Michell, D., Krimigis, S.M., Waite Jr., J.H., 2008. Energetic ion precipitation at Titan. Geophys. Res. Lett., 35, 03103, doi:10.1029/2007GL032451.

Cravens, T.E., et al., 2009. Model-data comparisons for Titan's nightside ionosphere. Icarus 199, 174–188.

English, M.A., Lara, L.M., Lorenz, R.D., Ratcli_, P., Rodrigo, R., 1996. Ablation and chemistry of meteoric materials in the atmosphere of Titan. Adv. Space Res. 17, 157–160.

Fortes, A.D., 2000. Exobiological implications of a possible ammonia-water ocean inside Titan. Icarus 146, 444–452.

Frencklach, M., 2002. Reaction mechanism of soot formation in flames. Phys. Chem. Chem. Phys. 4, 2028–2037.

Fulchignoni, M., Ferri, F., Angrilli, F., et al., 2005. In situ measurements of the physical characteristics of Titan's environment. Nature 438, 785–791.

Gerhardt, Ph., Löffler, S., Homann, K.H., 1987. Polyhedral carbon ions in hydrocarbon flames. Chem. Phys. Lett. 137 (4), 306–310.

Goulay, F., Rebrion-Rowe, C., arles, S., Le Garrec, J.L., Rowe, B.R., 2004. Electron attachment on HI and DI in a uniform supersonic flow: thermalization of the electrons. J. Chem. Phys. 121, 1303.

Goulay, F., Leone, S.R., 2006. Low-temperature rate coefficients for the reaction of ethynyl radical (CH) with benzene. J. Phys. Chem. 110 (5), 1875–1880.

Hanel, R.A., Conrath, B.J., Flasar, F.M., Kunde, V.G., Maguire, W., Pearl, J.C., Pirraglia, J.A., Samuelson, R., Hearth, L., Allison, M., Cruikshank, D.P., Gautier, D.,

Gierasch, C., Horn, L., Koppany, R., Ponnamperuma, C., 1981. Infrared observations of the Saturnian system from Voyager 1. Science 212, 192–200.

Hanel, R.A., Conrath, B.J., Flasar, F.M., Kunde, V.G., Maguire, W., Pearl, J.C., Pirraglia, J.A., Samuelson, R., Cruikshank, D.P., Gautier, D., Gierasch, P., Horn, L., Ponnamperuma, C., 1982. Infrared observations of the Saturnian system from Voyager 2. Science 215, 544–548.

Hartle, R.E., Sittler Jr., E.C., Ogilvie, K.W., Scudder, J.D., Lazarus, A.J., Atreya, S.K., 1982. Titan's ion exosphere observed from Voyager 1. J. Geophys. Res. 87, 1383.

Hartle, R.E., Sittler Jr., E.C., Neubauer, F.M., Johnson, R.E., Smith, H.T., Crary, F., McComas, D.J., Young, D.T., Coates, A.J., Simpson, D., Bolton, S., Reisenfeld, D., Szego, K., Berthelier, J.J., Rymer, A., Vilppola, J., Steinberg, J.T., Andre, N., 2006a. Preliminary interpretation of Titan plasma interaction as observed by the Cassini plasma spectrometer: comparisons with Voyager 1. Geophys. Res. Lett. 33, L08201, doi:10.1029/2005GL024817.

Hartle, R.E., Sittler Jr., E.C., Neubauer, F.M., Johnson, R.E., Smith, H.T., Crary, F., McComas, D.J., Young, D.T., Coates, A.J., Simpson, D., Bolton, S., Reisenfeld, D., Szego, K., Berthelier, J.J., Rymer, A., Vilppola, J., Steinberg, J.T., Andre, N., 2006b. Initial interpretation of Titan plasma interaction as observed by the Cassini plasma spectrometer: comparisons with Voyager 1. Planet. Space Sci. 54, 1211.

Hartle, R.E., Sittler Jr., E.C., Shappirio, M.D., Johnson, R.E., Luhmann, J.G., Ledvina, S.A., Cooper, J.F., Coates, A.J., Szego, K., Burger, M.H., Simpson, D.G., Crary, F., Young, D.T., 2006c. Saturn's magnetosphere ion erosion by Titan: penetration and loss of water group ionsin upper atmosphere. EOS Trans. AGU 87 (52) Fall Meet. Suppl., Abstract P13A-0161.

Hartle, R.E., Sittler Jr., E.C., Lipatov, A.S., 2008. Ion escape from the ionosphere of Titan. Geophys. Res. Abstr., Vol. 10, EGU2008-A-09860, 2008, SRef-ID: 1607-7962/gra/EGU2008-A-09860, EGU General Assembly.

Herbst, E., 1981. Can negative molecular ions be detected in dense interstellar clouds?. Nature 289, 656.

Herbst, E., Osamura, Y., 2008. Calculations on the formation rates and mechanisms for C_nH anions in interstellar and circumstellar media. Astrophys. J. 679, 1670–1679.

Hörst, S.M., Vuitton, V., Yelle, R.V., 2008. The origin of oxygen species in Titan's atmosphere. J. Geophys. Res., 113, E10006, doi:10.1029/2008JE003135.

Hunten, D.M., 1997. Titan's atmosphere and surface. In: Burns, J.A. (Ed.), Planetary Satellites. University of Arizona Press, Tucson, pp. 420–437.

Hunter, J.M., Fye, J.L., Roskamp, E.J., Jarrold, M.F., 1994. Isomerization of pure carbon cluster ions: From rings to fullerenes. In: Molecules and Grains in Space, AIP Conference Proceedings 312. Mont Sainte-Odile, France 1993, ed. Irène Nenner, pp. 571–588.

Ip, W.-H., 1990. Meteoroid ablation processes in Titan's atmosphere. Nature 345, 511–512.

Jaffke, T., Illenberger, E., Lezius, M., Matejcik, S., Smith, D., Märk, T.D., 1994. Formation of C_{60}^- and C_{70}^- by free electron capture. Activation energy and effect of the internal energy on lifetime. Chem. Phys. Lett. 226, 213–218.

Johnson, R.E., Liu, M., Sittler Jr., E.C., 2005. Plasma-induced clearing and redistribution of material embedded in planetary magnetospheres. Geophys. Res. Lett. 32, L24201, doi:10.1029/2005GL024275.

Kliore, A.J., Nagy, A.F., Marouf, E.A., French, R.G., Flasar, F.M., Rappaport, N.J., Anabttawi, A., Asmar, S.W., Kahann, D.S., Barbinis, E., Goltz, G.L., Fleischman, D.U., Rochblatt, D.J., 2008. First results from the Cassini Radio Occultations of the Titan ionosphere. J. Geophys. Res., 113, A09317, doi:10.1029/2007JA012965.

de Kok, R., Irwin, P.G.J., Teanby, N.A., Nixon, C.A., Jennings, D.E., Fletcher, L., Howett, C., Calcutt, S.B., Bowles, N.E., Flasar, F.M., Taylor, F.W., 2007. Characteristics of Titan's stratospheric aerosols and condensate clouds from Cassini CIRS far-infrared spectra. Icarus 191, 223–235.

Krätschmer, W., Lamb, L.D., Fostiropoulos, K., Huffman, D.R., 1990. Solid C_{60}: a new form of carbon. Nature 347, 354–358.

Kroto, H.W., Heath, J.R., O'Brien, S.C., Curl, R.F., Smalley, R.E., 1985. C_{60}: Buckminsterfullerene. Nature 318, 162–163.

Kroto, H.W., Allaf, A.W., Balm, S.P., 1991. C_{60}: Buckminsterfullerene. Chem. Rev. 91, 1213–1235.

Kuiper, G.P., 1944. Titan: a satellite with an atmosphere. Astrophys. J. 100, 378.

Lara, L.M., Lellouch, E., López-Moreno, J.J., Rodrigo, R., 1996. Vertical distribution of Titan's atmospheric neutral constituents. J. Geophys. Res. 101 (E10), 23261–23283.

Lavvas, P.P., Coustenis, A., Vardavas, I.M., 2008a. Coupling photochemistry with haze formation in Titan's atmosphere: Part I: Model description. Planet. Space Sci. 56, 27–66.

Lavvas, P.P., Coustenis, A., Vardavas, I.M., 2008b. Coupling photochemistry with haze formation in Titan's atmosphere, Part II: Results and validation with Cassini/Huygens data. Planet. Space Sci. 56, 67–99.

Liang, M-C., Yung, Y.L., Shemansky, D.E., 2007. Photolytically generated aerosols in the mesosphere and thermosphere of Titan. Astrophys. J. Lett. 661, L199–L202.

Lopes, R., Mitchell, K.L., Stofan, E.R., et al., 2007. Cryovolcanic features on Titan's surface as revealed by the Cassini Titan Radar Mapper. Icarus 186, 395–412.

Lorenz, R.D., et al., 2008. Titan's rotation reveals an internal ocean and changing zonal winds. Science 319, 1649–1651.

Luna, H., Michael, M., Shah, M.B., Johnson, R.E., Latimer, C.J., McConkey, J.W., 2003. Dissociation of N_2 in capture and ionization collisions with fast H^+ and N^+ ions and modeling of positive ion formation in the Titan atmosphere. J. Geophys. Res. 108101029/2002JE001950.

Lutz, B., de Bergh, C., Owen, T., 1983. Titan: discovery of carbon monoxide in its atmosphere. Science 220, 1374–1375.

MacLeod, J.M., Avery, L.W., Broten, N.W., 1984. The detection of interstellar methyldiacetylene (CH3C4H). Astrophys. J. 282, L89–L92.

Martin, T.P., Zimmermann, U., Malinowski, N., Heinebrodt, M., Frank, S., Tast, F., 1996. Clusters of fullerene molecules and metal atoms. Phys. Scr. T66, 38–47.

McCarthy, M.C., Gottlieb, C.A., Gupta, H., Thaddeus, P., 2006. Laboratory and astronomical identification of the negative molecularion C_6H^-. Astrophys. J. 652, L141–L144.

McKay, C.P., Smith, H.D., 2005. Possibilities for methanogenic life in liquid methane on the surface of Titan. Icarus 178 (1), 274–276.

Mebel, A.M., Kislov, V.V., Kaiser, R.I., 2008. Photoinduced mechanism of formation and growth of polycyclic aromatic hydrocarbons in low-temperature environments via successive ethynyl radical additions. J. Am. Chem. Soc. 130 (41), 13618–13629.

Michael, M., Johnson, R.E., 2005. Energy deposition of pickup ions and heating of Titan's atmosphere. Planet. Space Sci. 53, 1510–1514.

Michael, M., Johnson, R.E., Leblanc, F., Liu, M., Luhmann, J.G., Shemantovich, V.I., 2005. Ejection of nitrogen from Titan's atmosphere by magnetospheric ions and pickup ions. Icarus 175, 263–267.

Miller, T.J., Walsh, C., Cordiner, M.A., Ni Chumin, R., Herbst, E., 2007. Hydrocarbon anions in interstellar clouds and circumstellar envelopes. Astrophys. J. 662, L87–L90.

Mitchell, D.G., Brandt, P.C., Roelof, E.C., Dandouras, J., Krimigis, S.M., Mauk, B.H., 2005. Energetic neutral atom emissions from Titan interaction with Saturn's magnetosphere. Science 308, 989.

Molina-Cuberos, G.J., López-Moreno, J.J., Rodrigo, R., Lara, L.M., O'Brien, K., 1999. Ionization by cosmic rays of the atmosphere of Titan. Planet. Space Sci. 47, 1347–1354.

Molina-Cuberos, G.J., Lammer, H., Stumptner, W., Schwingenschuh, K., Rucker, H.O., López-Moreno, J.J., Rodrigo, R., Tokano, T., 2001. Ionospheric layer induced by meteoric ionization in Titan's atmosphere. Planet. Space Sci. 49, 143–153.

Moustefaoui, T., Rebrion-Rowe, C., Le Garrec, Jean-Luc, Rowe, B.R., Mitchell, J.B.A., 1998. Low temperature electron attachment to polycyclic aromatic hydrocarbons. Faraday Discuss. 109, 71–82.

Neish, C.D., Lorenz, R.D., O'Brien, D.P., 2006. The potential for prebiotic chemistry in the possible cryovolcanic dome Ganesa Macula on Titan. Int. J. Astrobiol. 5, 57–65.

Nelson, R.M., Kamp, L.W., Matson, D.L., et al., 2009. Saturn's Titan: surface change, ammonia, and implications for atmospheric and tectonic activity. Icarus 199, 429–441.

Ness, N.F., Acuna, M.H., Lepping, R.P., Connerney, J.E.P., Behannon, K.W., Burlaga, L.F., Neubauer, F.M., 1981. Magnetic field studies by Voyager 1: preliminary results at Saturn. Science 212, 211.

Petrie, S., Bohme, D.K., 2007. Ions in space. Mass Spectrom. Rev. 26, 258–280.

Raulin, F., 2008. Organic lakes on Titan. Nature 454, 587–589.

Raulin, F., Owen, T.C., 2003. Space Sci. Rev. 104, 377–394.

Remijan, A.J., Hollis, J.M., Snyder, L.E., Jewell, P.R., Lovas, F.J., 2006. Methyltriacetylene (CH3C6H) toward TMC-1: the largest detected symmetric top. Astrophys. J. 643, L37–L40.

Remijan, A.J., Hollis, J.M., Lovas, F.J., Cordiner, M.A., Millar, T.J., Markwick-Kemper, A.J., Jewell, P.R., 2007. Detection of C_8H^- and comparison with C_3H toward IRC +10 216. Astrophys. J. 664, L47–L50.

Ricca, A., Bauschlicher Jr., C.W., Bakes, E.L.O., 2001. A computational study of the mechanisms for the incorporation of a nitrogen atom into polycyclic aromatic hydrocarbons in the Titan haze. Icarus 154, 516–521.

Richter, H., Howard, J.B., 2000. Formation of polycyclic aromatic hydrocarbons and their growth to soot—a review of chemical reaction pathways. Prog. Energy Combust. Sci. 26, 565–608.

Roe, H.G., de Pater, I., MacIntosh, B.A., McKay, C.P., 2002. Titan's clouds from Gemini and Keck adaptive optics imaging. Astrophys. J. 581, 1399–1406.

Sagan, C., Khare, B.N., 1979. Tholins—organic chemistry of interstellar grains and gas. Nature 277, 102–107.

Sakai, N., Sakai, T., Yamamoto, S., 2007. Detection of C_6H^- toward the low-mass protostar IRAS 04368+2557 in L1527. Astrophys. J. 667, L65–L68.

Sakai, N., Sakai, T., Yamamoto, S., 2008. Tentative detection of C_4H^- toward the low-mass protostar IRAS 04368+2557 in L1527. Astrophys. J. 673, L71–L74.

Samuelson, R.E., Maguire, W.C., Hanel, R.A., Kunde, V.G., Jennings, D.E., Yung, Y.-L., Aikin, A.C., 1983. CO_2 on Titan. J. Geophys. Res. 88, 8709.

Schlesinger, W.H., 1997. Biogeochemistry: An Analysis of Global Change. Academic Press, San Diego, p. 302.

Shah, M.B., Latimer, C.J., Montenegro, E.C., Tucker, O.J., Johnson, R.E. and Smith, H.T., The implantation and interactions of O^+ in Titan's atmosphere: laboratory measurements of collision-induced-dissociation in N_2 and the modeling of positive ion formation. ApJ. (2009) in press.

Shemansky, D.E., Stewart, A.I.F., West, R.A., Esposito, L.W., Hallett, J.T., Liu, X.M., 2005. Science 308, 978.

Sittler Jr., E.C., Hartle, R.E., Vinas, A.F., Johnson, R.E., Smith, H.T., Mueller-Wodarg, I., 2004. Titan interaction with Saturn's magnetosphere: mass loading and ionopause location. In: Proceedings of the International Conference TITAN From Discovery to Encounter, ESA Spec. Publ. 1278, p. 377, ESTEC, Noordwijk, Netherlands.

Sittler Jr., E.C., Hartle, R.E., Vinas, A.F., Johnson, R.E., Smith, H.T., Mueller-Wodarg, I., 2005. Titan interaction with Saturn's magnetosphere: Voyager 1 results revisited. J. Geophys. Res. 110, A09302, doi:10.1029/2004JA010759.

Sittler Jr., E.C., Johnson, R.E., Smith, H.T., Richardson, J.D., Jurac, S., Moore, M., Cooper, J.F., Mauk, B.H., Michael, M., Paranicus, C., Armstrong, T.P., Tsurutani, B., 2006. Energetic nitrogen ions within the inner magnetosphere of Saturn. J. Geophys. Res. 111, A09223, doi:10.1029/2004JA010509.

Sittler Jr., E.C., et al., 2008. Ion and neutral sources and sinks within Saturn's inner magnetosphere: Cassini results. Planet. Space Sci 56, 3–18.

Sittler Jr., E.C., Hartle, R.E., Lipatov, A.S., Cooper, J.F., Bertucci, C., Coates, A.J., Szego, K., Johnson, R.E., Shappirio, M., Simpson, D.G., Wahlund, J.-E., 2009. Saturn's magnetospheric Interaction with Titan as defined by Cassini Encounters T9 and T18: new results. Planet. Space Sci. submitted.

Smith, D., Spanel, P., Märk, T.D., 1993. Electron attachment to C_{60} at low energies. Chem. Phys. Lett. 213 (1/2), 202–206.

Smith, I.W.M., Rowe, B.R., 2000. Reaction kinetics: at very low temperatures: laboratory studies and interstellar chemistry. Acc. Chem. Res. 33 (5), 261–268.

Smith, I.W.M., Sage, A.M., Donahue, N.M., Herbst, E., Quan, D., 2006. The temperature-dependence of rapid low temperature reactions: experiment, understanding and prediction. Faraday Discuss. 133, 137–156.

Sotin, C., Jaumann, R., Buratti, B.J., et al., 2005. Release of volatiles from a possible cryovolcanic from near-infrared imaging of Titan. Nature 435, 786–789, doi:10.1038/nature03596.

Spanel, P., Smith, D., 1994. A study of electron attachment to C_{76} using the FALP technique. Chem. Phys. Lett. 229, 262–266.

Spanel, P., Smith, D., 1995. Recent studies of electron attachment and electron-ion recombination at thermal energies. Plasma Sources Sci. Technol. 4, 302–306.

Srama, R., Kempf, S., Moragas-Klostermeyer, G., Helfert, S., Ahrens, T.J., Altobelli, N., Auer, S., Beckmann, U., Bradley, J.G., Burton, M., Dikarev, V.V., Economou, T., Fechtig, H., Green, S.F., Grande, M., Havnes, O., Hillier, J.K., Horanyi, M., Igenbergs, E., Jessberger, E.K., Johnson, T.V., Kruger, H., Matt, G., McBride, N., Mocker, A., Lamy, P., Linkert, D., Linkert, G., Lura, F., McDonnell, J.A.M., Möhlmann, D., Morfill, G.E., Postberg, F., Roy, M., Schwehm, G.H., Spahn, F., Svestka, J., Tschernjawski, V., Tuzzolino, A.J., Wäsch, R., Grün, E., 2006. In situ dust measurements in the inner Saturnian system. Planet. Space Sci. 54, 967–987.

Stiles, B.W., Hensley, S., Gim, Y., et al., 2009. Icarus 202 (2), 584–598.

Stofan, E. R., Elachi, C., Lunine, J. I., et al., 2007. The lakes of Titan. Nature 441, 61–64, doi:10.1038/nature05438.

Thaddeus, P., 1994. On the large organic molecules in the interstellar gas. In: Irène Nenner (Ed.), Molecules and Grains in Space, AIP Conference Proceedings 312, Mont Sainte-Odile, France 1993, pp. 711–731.

Thaddeus, P., 1995. Carbon chains and the diffuse interstellar bands. In: Tielens, A.G.G.M., Snow, T.P. (Eds.), The Diffuse Interstellar Bands. Kluwer Academic Publishers, The Netherlands, pp. 369–378.

Thaddeus, P., Gottlieb, C.A., Gupta, H., Brünken, S., McCarthy, M.C., Agúndez, M., Guélin, M., Cernicharo, J., 2008. Laboratory and astronomical detection of the negative molecular ion C_3N^-. Astrophys. J. 677, 1132–1139.

Tobie, G., Grasset, O., Lunine, J.I., Mocquet, A., Sotin, C., 2005. Titan's internal structure inferred from a coupled thermal-orbital model. Icarus 175, 496–502.

Tomasko, M., et al., 2005. Rain, winds and haze during Huygens probe's descent to Titan's surface. Nature 438 (8), 765–778.

Toublanc, D., Parisot, J.P., Gautier, D., Raulin, F., McKay, C.P., 1995. Photochemical modeling of Titan's atmosphere. Icarus 113, 2.

Vuitton, V., Yelle, R.V., McEwan, M.J., 2007. Ion chemistry and N-containing molecules in Titan's upper atmosphere. Icarus 191, 722.

Vuitton, V., Yelle, R.V., Lavvas, P., 2009a. Composition and chemistry of Titan's thermosphere and ionosphere. Phil. Trans. R. Soc. A 367, 729–741.

Vuitton, V., Lavvas, P., Yelle, R.V., Galand, M., Wellbrock, A., Lewis, G.R., Coates, A.J., Wahlund, J.-E., 2009b. Negative ion chemistry in Titan's upper atmosphere. Planet. Space Sci., in press, doi:10.1016/j.pss.2009.04.004.

Wahlund, J.-E., et al., 2005. Cassini measurements of cold plasma in the ionosphere of Titan. Science 308, 986–989.

Wahlund, J.-E., Galand, M., Müller-Wodarg, I., Cui, J., Yelle, R.V., Crary, F.J., Mandth, K., Magee, B., Waite Jr., J.H., Young, D.T., Coates, A.J., Garnier, P., Ågren, K., André, M., Eriksson, A.I., Cravens, T.E., Vuitton, V., Gurnett, D.A., Kurth, W.S., 2009. On the amount of heavy molecular ions in Titan's ionosphere. Planet. Space Sci., in press, doi:10.1016/j.pss.2009.07.014.

Waite, J.H., et al., 2005. Ion neutral mass spectrometer results from the first flyby of Titan. Science 308, 982–986.

Waite Jr., J.H., Young, D.T., Cravens, T.E., Coates, A.J., Crary, F.J., Magee, B., Westlake, J., 2007. The process of Tholin formation in Titan's upper atmosphere. Science 316, 870, doi:10.1126/science.1139727.

Waite Jr., J.H., Young, D.T., Coates, A.J., Crary, F.J., Magee, B.A., Mandt, K.E., Westlake, J.H., 2008. The Source of Heavy Organics and Aerosols in Titan's Atmosphere. 2008, IAU: Organic Matter in Space, IAU Symposium and Colloquium Proceedings Series, no. 251, pp. 321–326.

Wang, L.S., Conceicao, J., Jin, J., Smalley, R.E., 1991. Threshold photodetachment of cold C_{60}-. Chem. Phys. Lett. 182, 5.

Wang, X.B., Woo, H.K., Wang, L.S., 2005. Vibrational cooling in a cold ion trap: Vibrationally resolved photoelectron spectroscopy of cold C_{60}- anions. J. Chem. Phys. 123, 051106, doi:10.1063/1.1998787.

Weiske, T., Bohme, D.K., Schwarz, H., 1991. Injection of helium atoms into doubly and triply charged C_{60} cations. J. Phys. Chem. 95, 8451–8452.

Wilson, E.H., Atreya, S.K., 2004. Current state of modeling the photochemistry of Titan's mutually dependent atmosphere and ionosphere. J. Geophys. Res. 109, E06002, doi:10.1029/2003JE002181.

Yang, S.H., Pettiette, C.L., Conceicao, J., Cheshnovsky, O., Smalley, R.E., 1987. Chem. Phys. Lett. 139, 233.

Yung, Y.L., 1987. An update of nitrile photochemistry on Titan. Icarus 72, 468.

Yung, Y.L., Allen, M., Pinto, J.P., 1984. Photochemistry of the atmosphere of Titan: comparison between model and observations. Astrophys. J. Suppl. 55, 465.